Multi-mode relaying for energy consumption reduction

Cédric Lévy-Bencheton, Doreid Ammar, Guillaume Villemaud, Tanguy Risset, Clément Reboul

INRIA

INSTITUT NATIONAL DE RECHERCHE EN INFORMATIQUE ET EN AUTOMATIQUE

Multi-mode relaying for energy consumption reduction

Cédric LÉVY-BENCHETON — Doreid AMMAR — Guillaume VILLEMAUD — Tanguy RISSET — Clément REBOUL

N° 7245

Octobre 2010

Domaine 3

ISSN 0249-6399 ISRN INRIA/RR--7245--FR+ENG

INSTITUT NATIONAL
DE RECHERCHE
EN INFORMATIQUE
ET EN AUTOMATIQUE

INRIA

centre de recherche
GRENOBLE - RHÔNE-ALPES

Multi-mode relaying for energy consumption reduction

Cédric LÉVY-BENCHETON*†, Doreid AMMAR*† , Guillaume VILLEMAUD*† , Tanguy RISSET*† , Clément REBOUL*†

Domaine : Réseaux, systèmes et services, calcul distribué
Équipe-Projet SWING

Rapport de recherche n° 7245 — Octobre 2010 — 28 pages

Abstract: Today mobile terminals offer today the possibility of switching between different physical layers of radio protocols. With a generalization of Software Defined Radio, this multi-mode property improves the connectivity but has an important cost in terms of energy consumption. In this paper, we study the possibility of reducing energy consumption by using a relay on possibly different communication modes.

We show that a multi-mode relay, compared to simple (mono-mode) relay, has an impact on energy consumption. We propose an analytical study of energy consumption in multi-mode terminals. Then, we will compare the network energy consumption following two scenarios: in the first one, a mobile terminal relays other users, in the second one terminals connect directly to an Access Point. We evaluate the consumption of the terminals in an 802.11g-to-UMTS and an 802.15.4-to-802.11g relay scheme. We isolate rules to minimize the network global energy consumption through multi-mode relaying. We show that the most intuitive solution is not always the best one and that a very precise simulation is necessary to make good choices at run time.

Key-words: multi-mode relay, software defined radio, energy evaluation, energy reduction, simulation

* Université de Lyon, INRIA
† INSA-Lyon, CITI, F-69621, France

Centre de recherche INRIA Grenoble – Rhône-Alpes
655, avenue de l'Europe, 38334 Montbonnot Saint Ismier
Téléphone : +33 4 76 61 52 00 — Télécopie +33 4 76 61 52 52

Relai multi-mode dans un but de réduction de la consommation d'énergie

Résumé : Aujourd'hui, les terminaux mobiles permettent de choisir parmi différentes couches physiques de protocoles radios. Avec la généralisation de la Radio Logicielle, cette propriété multi-mode améliore la connectivité, mais rajoute un important surcoût à la consommation d'énergie. Dans ce papier, nous étudions la possibilité de réduire la consommation d'énergie en proposant un relais peut communiquer sur ces différents modes.

Nous montrons qu'un relais multi-mode a un impact sur la consommation d'énergie, en comparaison à un simple relais mono-mode. Nous proposons une étude analytique de la consommation d'énergie pour les terminaux multi-modes. Puis, nous comparons la comsommation d'énergie du réseau suivant deux scénarios: dans le premier, un terminal mobile joue le rôle de relais pour d'autres utilisateurs ; dans le second, tous les terminaux se connectent directement au point d'accès. Nous évaluons la consommation des terminaux dans des scénarios de relais 802.11g-vers-UMTS et 802.15.4-vers-802.11g. Nous isolons des règles qui permettent de minimiser la consommation global du réseau au travers des relais multi-modes. Nous montrons que la solution la plus intuitive n'est pas toujours la meilleure, et qu'une évaluation précise au travers de simulations est nécessaire afin de procéder à un bon choix de paramètres.

Mots-clés : relai multi-mode, radio logicelle, réduction d'énergie

Contents

1 Introduction

Today, more and more mobile applications require permanent network connectivity. Current mobile terminals provide several communications *protocols*, such as WiFi [15] and UMTS [1]. These different protocols can be implemented by several hardware circuit or by reconfiguring a common hardware platform such as in the Software Defined Radio (SDR) paradigm. In addition, each protocol can, to a certain extent, chose between different configurations for some of the parameters: coding rate, modulation, etc. We refer to such terminals as *multi-mode* terminals.

An interesting property appeared recently on multi-mode terminals: their ability to rapidly change the radio protocol used. This offers the possibility of choosing a communication mode according to a particular objective: quality of Service, users' preferences, access cost, or energy reduction. In practice, this flexibility comes with an increasing energy consumption. Although mobile terminals provide larger batteries, we observe little to no gain on their average lifetime. Furthermore, the network energy consumption keeps rising, and operators are eager for new solutions to reduce these costs.

Current devices rely on a number of dedicated chipsets to provide multi-mode radio interface. With one chipset associated to one mode, the terminal cost and energy consumption are rising drastically. One solution lies in Software Defined Radio, where the multiple chipsets found in current devices are replaced by a single generic purpose processor running algorithms. Thus, a multi-mode SDR implements different modes as different algorithms. Since all modern protocols share commonalities, these algorithms are reusable between modes. This leads to a facilitated implementation of new modes, better efficiency of parallel communications in several modes, and improvements in performances and energy.

Still, SDR does not solve all problems. How can operators ensure permanent network connectivity without increasing costs? *Relaying* communication is a way to minimize cost and energy consumption. A *relay* is a device transmitting data from another user device to an access point. The use of such a relay permits the user to emit at a lower energy mode. Such relays can be deployed by operators or be mobile. In the latter case, the users' terminals act as potential relays.

In this work, we present an analysis of multi-mode terminals energy consumption. We propose a careful study of all elements (related to the physical layer) involved in radio protocols energy consumption. We first evaluate the algorithmic complexity for different communication protocols, which is closely related to the energy consumption in an SDR. We focus on the IEEE 802.11g (WiFi) [15], a WLAN standard, 3GPP UMTS [1], a voice and data long-range mobile communication mode, and the IEEE 802.15.4, or Zigbee, a low-power WPAN [16].

We study how the multi-mode possibility can be used in order to reduce the network global energy consumption through relay schemes. As opposed to existing works on relaying, we study not only the transmission power but also numerical and analogical energy consumptions. Our hypothesis is that, for a given terminal, energy consumption induced by upper communication layer (network, application) will be negligible in comparison with the physical layer, although this does not mean that these protocols cannot improve global network performance.

Evaluating energy consumption when an important number of terminals are concerned is a difficult task. It must be done by simulation (analytical modelling is still too imprecise) and the simulated scenario must be sufficiently simple to provide meaningful information.

We propose a review of the SDR paradigm and introduce our approach to reduce energy consumption in section 2. We present the algorithmic complexity of the protocols under study in section 3. Then, we present an analytical energy model for energy consumption in radio communication protocols in section 4. We explain how to evaluate the numerical and analog energy consumption for different channel models. Section 5 introduces the global energy consumption, together with the different scenarios used in its evaluation. We realize Matlab simulations on 802.11g-to-UMTS relay as presented in section 6. These result highlight the fact that a more realistic approach is needed for evaluating the global energy consumption of 802.15.4-to-802.11g relay. This was done in section 7 where we take into account the energy cost of network control packets and passive overhearing in the WSNet network simulator [9]. Finally, we synthesize the results to isolate the need for a realistic study to predict the behaviour of energy consumption in a multi-mode relay in section 8.

2 Software defined radio and relays, leading to a lower energy consumption

2.1 State of the art

We review work done on the potential benefits obtained by relays and SDR, focusing particularly on energy savings.

At the physical layer level, Inwhee et al. ([18]) select the least consuming mode with an algorithm taking into account the required quality of service, the cost for the user and remaining battery life of the terminal. The authors rely on realistic radio energy consumption values to evaluate the terminal consumption but do ignore the energy consumption from the digital part.

A terminal can also benefit from multi-mode in a context of ubiquitous services as presented in [8]. The paper expresses the necessity of energy reduction in a pervasive service discovery scheme, by reconfiguring a multi-mode terminal to communicate on the most energy efficient interface. However, the choice is not only led by the lowest energy consumption, but also needs to take into account the service type. The authors identified that a “low-power" standard (here Bluetooth) is actually not the less consuming mode, due to a higher consumption per packet. However, they do not consider relaying.

As mentioned before, SDR provides the adaptability required to switch protocol dynamically. Different research enhances and facilitates the terminal reconfiguration. Berlemann et al. implement a realistic protocol stack, sharing processing blocks between 802.11g and UMTS [5]. This work is more focused on the network access and transport layers, instead of the physical layer. This gap is filled by Montium, a low-power SDR architecture, sharing processing blocks between different parallel modes [26]. Montium can be at the core of mobile SDR terminals, but requires specific programming for the different communication protocols. Again, multi-mode is not evaluated.

An SDR has reconfiguration capabilities, which brings the flexibility needed to guarantee a permanent connection. This reconfiguration could be guided by a metric based on different criteria. Classical metrics are based on the communication channel conditions as in [11], where the reception mode is chosen according to Signal to Noise Ratio. But long term energy savings are not guaranteed in these approaches. Ganesan and Li propose a local metric, computed at the terminal, to evaluate interference caused

by cognitive users for a primary user, both communicating on a licensed frequency [12]. When the primary user is detected, cognitive users negotiate with each other to change communication mode. Reconfiguration is at the centre of the IEEE SCC41 Working Group [17], via P1900.4 [13]. Their proposal is to send a small packet, the radio enabler, containing all the needed information for the mobile terminal to select the best suitable network (number of operations per second, frequency, data bit rate, and so on). This work will enable operators to develop power reduction strategies based on multi-mode software tuning.

The energy consumption cannot be reduced only at the terminal. Relaying allows users to connect to closer access points in the case of fixed relays, or to share their connection in the case of mobile relays. Jiang et al. present a network of self-organized stations, which can act as fixed relays [20]. To prevent handover process near cell border, different fixed relays communicate with the cellular network to evaluate the need of relaying a mobile user. This proposal reduces the radio transmission power and interference, but it does not treat multi-mode.

Cavalcanti et al. present an heterogeneous multi-hop mobile wireless network [7]. In this network, mobile users can use other users' terminals as a relay to contact the access point through multi-hop communication. An algorithm estimates the "connectivity opportunity" from user preferences, required data rate and channel conditions. Cavalcanti et al. showed an improvement on network capacity and error rate but give no estimation on the energy consumption.

Wang et al. increase a sensor network lifetime of up to four times thanks to mobile relays [31] using a reduced transmission power between relays. Relays are simple sensors with a larger battery. Mobile relays provide a better network autonomy, reduction of capacity bottlenecks, cost savings and more importantly, the normal behaviour of the mobile sensor when not acting as a relay.

Seddik et al. minimized the outage probability by dynamically adjusting the transmissions power values in Amplify-and-Forward multi-relay networks [27]. Their adaptive strategies bring a larger energy reduction than classical power allocation approaches, and at any distance from the access point, thanks to relaying. Nourizadeh et al. expose the advantages and disadvantages of mobile relays: greater network capacity, lower consumption when relaying a single user and also cost savings in network deployment for an equivalent user satisfaction [25].

In cooperative clusters, terminals share their connections through adapted strategies. They improve personal gains while reducing the network energy consumption [2, 3]. These works explore multi-mode communication: they allow communications on selected modes inside the cluster, and on a particular mode with the access point. However, the authors only use radio transmission power, and do not consider multi-mode in the gain provided to multi-users.

In a network where all terminals are similar, relays may ensure energy efficiency. For example, Madan et al. relied on channel conditions to minimize the global energy consumption using cooperation [23]. In a similar approach, Hwang and Ko increase the network lifetime with periodical channel measurements [14]. In sensor networks, multi-hop relaying reduces the global energy consumption while maximizing the network lifetime [22].

2.2 Our approach

Compared to works presented above, our work proposes a more precise modelling of the multi-mode relay scenario. We propose a precise simulation, for the terminal, i.e

including numerical complexity in the terminal energy consumption, as well as for the protocol behaviour, i.e. taking into account control packets and passive overhearing for instance.

Control packets provide a fair access to the medium; they are part of the MAC layer and are often "forgotten" in network simulators. Passive overhearing occurs when a terminal receives a signal from other terminals which is not destined to him. We focus on the physical layer, including the numerical and analogical energy consumption, unlike classical relay works which only take into account the radio transmission power. The scope of this paper being the physical layer energy consumption, it does not consider upper layers in the energetic estimation.

An SDR implements a mode via software blocks, so we study the algorithmic complexity of the software blocks of 802.11g, UMTS and 802.15.4 protocols for a given terminal. In order to compare different modes, with different transmission rate, we must compare the energy consumed *per bit of useful data transmitted*. Hence we evaluate the software complexity and, given the number of data bits transmitted, deduce the terminal numerical energy consumption per bit of data transmitted. Then, we compute the radio consumption per bit for every mode. Based on these two values: numerical and radio energy consumption, we can select the most efficient mode and minimize the terminal energy consumption.

In our scenario, we combine several of these SDR terminals to form a multi-mode relay scheme. One Primary Users (denoted PU), whose terminal can act as a relay for one or several Secondary User(s) (denoted SU). The PU is in communication with an Access Point (or equivalently a base station) denoted AP. In a first evaluation, we use Matlab simulations. The Matlab simulations have a coarser precision: they do not include passive overhearing or interference. In these simulations, we compare the energy consumption of communication between SU and AP, with and without relaying through PU. We perform these comparisons, for 802.11g-to-UMTS and 802.15.4-to-802.11g relays. The results have highlighted the presence of a "No-Relay Zone": a zone where relaying has no positive impact on global energy consumption. Then, we express rules to minimize the global energy consumption with multi-mode relaying.

However, performing more precise simulations has shown that these rules are not applicable in the case of an 802.15.4-to-802.11g relay. This is due to the cost induced by MAC layer control packets and passive overhearing. Hence, we propose a more realistic evaluation, by relying on a network simulator. We have used WSNet, a realistic wireless network simulator developed at the CITI Laboratory [9]. WSNet is an open-source simulator providing realistic PHY and MAC layers, with a modular interface allowing rapid development of add-ons, coded in C. To perform our simulations, we have designed multi-mode WSNet plug-ins and extended the energy module by integrating the numerical consumption for each mode.

3 Algorithmic Complexity study

A multi-mode SDR concurrently runs different algorithms corresponding to the physical layer, MAC layer, and upper layers of different radio protocols. Our energy model is composed of two parts: the *numerical energy*, i.e. energy used in all baseband and signal processing done by the generic processor, and the *radio energy* (or analog energy). On an SDR, each mode is split into two parts: the numerical part contains the processor and the algorithms, and the analogical part represents the radio frequency front-end. In this section, we evaluate the precise numerical energy which is tightly

Table 1: Parameters chosen for the algorithmic complexity evaluation of the different radio modes under study

	802.11g	
Data bitrate	6 Mbps	54 Mbps
Carrier frequency	2,400 Mhz	
Physical layer	OFDM	
Encoding	Convolutional (rate 1/2)	Convolutional (rate 3/4)
Modulation	BPSK	64-QAM
Number of carrier	64 subcarriers (48 data, 4 pilots, 12 null)	
Spreading factor	-	
Chips per second	-	
Frame size (bits)	$1,500 \times 8$	
Header size (bits)	30×8	

	UMTS	**802.15.4**
Data bitrate	384 kbps	20 kbps
Carrier frequency	1,900 Mhz (uplink) & 2,100 Mhz (downlink)	868 Mhz
Physical layer	Spreading & scrambling	Spreading
Encoding	Convolutional (rate 1/2)	Differential
Modulation	QPSK	BPSK
Number of carrier	1	1
Spreading factor	4	15
Chips per second	3.84 M	300 k
Frame size (bits)	3840	133×8
Header size (bits)	90 (DCCH: control channel)	8×8

linked to the algorithmic complexity of software treatments, for the different building blocks of 802.11g, 802.15.4 and UMTS.

3.1 A per-bit complexity analysis

The numerical complexity of a mode mostly depends on a set of parameters (*i.e.* modulation, code rate, ...). Complex bit transformations such as coding, spreading or modulation mapping lead to a high numerical complexity. For each mode, the SDR performs different steps in transmission, where data bits are transformed, coded, modulated, assembled into frames, and sent to a receiver at a given radio bitrate. The comparison of modes requires a common basis, especially between different communication protocols. Hence, we take into account all operations encountered by single data bit by each mode, and compute the number of operations per (data) bit.

3.2 Algorithmic complexity evaluation

In this section, we proceed to a careful study of the physical layer for chosen modes: 6 Mbps and 54 Mbps in 802.11g, 384 kbps in UMTS, and 20 kbps in 802.15.4. In order to estimate the numerical energy consumption, we define the *bitop* as the number of operations per bit. Although these modes share common operations, their bitop is highly dependent on the parameters used in each mode. Table 1 sums up the different parameters used to compute the algorithmic complexity of each mode. Table 2 presents

Table 2: Detailed algorithmic complexity for selected communication modes, in operation per bit (bitop)

TRANSMISSION

802.11g	**6 Mbps**	**54 Mbps**	**UMTS**	**384 kbps**	**802.15.4**	**20 kbps**
Scrambling	18	18	Cyclic Redundancy Check	6	Coding	4
Coding	74	66	Coding	83	Spreading	15
Puncturing	0	26	Puncturing	18	Mapping	75
Interleaving	11	7	First interleaving	0		
Mapping	10	3	Frame segmentation	7		
IFFT	195	22	Rate matching	7		
			Multiplexing	253		
			Second interleaving	80		
			Orthogonal Spreading	20		
			Scrambling	80		
			Mapping	60		
			DCCH	131		
TOTAL TX	**308**	**142**	**TOTAL TX**	**745**	**TOTAL TX**	**94**

RECEPTION

802.11g	**6 Mbps**	**54 Mbps**	**UMTS**	**384 kbps**	**802.15.4**	**20 kbps**
FIR filtering	680	76	FIR filtering	2,040	FIR filtering	1,620
Interpolation & decimation	2,467	275	Interpolation & decimation	1,850	Interpolation & decimation	975
Frequency adjustment	18	18	Slot synchronization	301	Frequency adjustment	2
Phase correction	2	2	Frame synchronization	36	Phase correction	2
Correlation	14	14	Descrambling	322	Correlation	1
FFT	195	22	Rake	80	Demapping	75
Demapping	10	3	DeMapping	60	Despreading	15
Deinterleaving	11	11	Second deinterleaving	80	Differential decoding	4
Depuncturing	0	26	Demultiplexing	253		
Viterbi decoding	155	188	Rate matching	7		
Descrambling	18	18	Frame desegmentation	7		
			First deinterleaving	0		
			Depuncturing	18		
			Viterbi Decoding	248		
			CRC	6		
TOTAL RX	**3,570**	**653**	**TOTAL RX**	**5,308**	TOTAL RX	**2,694**

the bitop for the protocols under study based on the work of Neel et al. in [24]. Before analysing the values, we briefly recall the use of each part of the protocols.

In transmission (TX), coding adds redundancy and interleaving randomizes bits position, in order to overcome errors introduced by the channel. Beforehand, UMTS applies an additional Cyclic Redundancy Check (CRC) at reception to verify data integrity. After mapping the coded bits into modulation symbols, the process differs for each protocol. In 802.11g, the signal is transmitted following Orthogonal Frequency-Division Multiplexing (OFDM): this techniques transmits data on orthogonal sub-carriers in order to attain a high rate with reduced bandwidth. OFDM transformation requires an Inverse Fast Fourier Transform (IFFT) which distributes data accordingly. On the contrary, UMTS and 802.15.4 spread the signal over a larger bandwidth. This operation allows signal decoding in the presence of a strong ambient noise.

In reception (RX), the terminal selects the interesting part of the analogical signal through a Finite Impulse Response (FIR) filter. This signal is then corrected and amplified through different operations which aim to recover the transmitted data. Several inverse operations have a similar complexity, such as the 802.11g Fast Fourier Transform (FFT) which reassembles data from the different sub-carriers. On the other hand, few operations increase the bitop due to their high complexity, like the Rake demodulator in UMTS or the Viterbi decoding in both 802.11g and UMTS.

Table 2 presents the bitop (rounded to the upper integer) for each components of 802.11g, UMTS and 802.15.4, for transmission and reception. The resulting bitop is based on the evaluation of the complexity presented by Neel et al. in [24]. The number of operation for each block is first evaluated per frame (a necessary step in certain operations), before being converted into bitop and rounded to the upper integer. Additional overheads are also part of the bitop computation: UMTS relies on a Dedicated Control Channel (DCCH) to indicate transmission parameters, whereas 802.11g and 802.15.4 use the frame header.

By analysing the results, it is shown that the highest bitop comes from the reception area. This behaviour is due to the algorithms allowing the receiver to recover a good signal quality. When comparing the different modes with each other, UMTS has the highest bitop, followed by 802.11g at 6 Mbps, 802.15.4 at 20 kbps and 802.11g at 54 Mbps. We notice that slow modes do not always guarantee a smaller bitop than faster modes. We explain this behaviour by the differences of each physical layer.

In each mode, the signal processing operations (FIR filtering, interpolation and decimation) represent the most expensive bitop. However, these operations have a lower bitop in 802.11g at 54 Mbps, which features more data bits than 6 Mbps for the same bandwidth. We now review other operations with high computational cost for all modes.

In 802.11g, the highest bitops come from the convolutional encoding and the IFFT in transmission, and from the Viterbi decoding and FFT in reception. Moreover, the modulation leads 54 Mbps to have a lower bitop than 6 Mbps. Indeed, 6 Mbps relies on a Binary Phase Shift Keying (BPSK) modulation, with one modulation symbol for one (coded) bit, whereas 54 Mbps uses a 64 symbols Quadrature Amplitude Modulation (64-QAM) with one transmitted symbol representing 6 coded bits.

In UMTS at 384 kbps, the high number of memory access for multiplexing gives a high bitop. The same applies to descrambling and Viterbi decoding, which represent a major complexity in reception. In addition, the Rake complexity increases with the spreading factor.

In 802.15.4, the mapping cost is largely induced by the high spreading factor. All other operations have very low processing requirements.

4 Energy consumption estimation

In multi-mode, a terminal's energy is divided between all its active modes. For this purpose, the first step is to evaluate the required energy for each implemented mode, in transmission (TX) and reception (RX). With each mode leading to different packet sizes, MAC and PHY layers, our evaluation focuses on the energy consumed during the transmission/reception of one single data bit.

We now define the *energy per bit*, E_{bit}, as the total energy required for a terminal to transmit or receive one single data bit in a chosen mode. As explained before, the terminal energy consumption is divided into two parts: E_{num}, the numerical energy consumption, and E_{rf}, the radio energy consumption. E_{num} depends on the algorithmic complexities and the processor architecture. E_{rf} is associated with the radio front-end architecture and the transmission power output (linked to the channel conditions). Hence:

$$E_{\text{bit}} = E_{\text{num}} + E_{\text{rf}} \tag{1}$$

4.1 Numerical energy consumption

In this section, we explain how to evaluate the numerical energy consumption, E_{num}, expressed in Joule per bit. The numerical energy consumption, denoted $E_{\text{num}}(K)$, is the energy consumed by the processor to realize K operations, in Joule per bit [29]:

$$E_{\text{num}}(K) = K\, E_{\text{cpu}} = K\, A_C\, V_{dd}^2 \tag{2}$$

where K is the bitop as defined in Section 3.2, and $E_{\text{cpu}} = A_C\, V_{dd}^2$ (in Joule) depends on the architecture of the terminal. A_C (in Farad), is the processor switching capacitance, and V_{dd} (in Volt) is the processor input voltage.

4.2 Radio energy consumption

The radio energy consumption, E_{rf}, in Joule per bit, depends on the radio-frequency front-end architecture (and its activity), and the transmission power. The transmission power, denoted P_{out}, depends on the mode specification and the channel conditions. Since both P_{frontend} and P_{out} are analogical, E_{rf} is time-related.

The radio energy consumption, E_{rf} (in Joule per bit), reduces as follows from [28]:

$$E_{\text{rf}} = \frac{1}{R}(P_{\text{frontend}} + \theta P_{\text{out}}) \tag{3}$$

with R the mode data bitrate (in bit per second), P_{frontend} (in Watt), the radio front-end architecture consumption, and P_{out} (in Watt), the radio transmission power output, and $\theta = 1$ in transmission, 0 otherwise. Since $\frac{1}{R}$ represents the time to send or receive one data bit, E_{rf} is in Joule per bit as stated before. P_{frontend} depends on the front-end specifications. In general, it remains fixed for a mode, with different values in transmission and reception. We also explain how to evaluate P_{out} in section 4.4, as a function of channel conditions.

4.3 Channel conditions

The terminals send data over the air in the form of an analog signal. This signal suffers channel conditions caused by the surrounding environment, such as pathloss, noise,

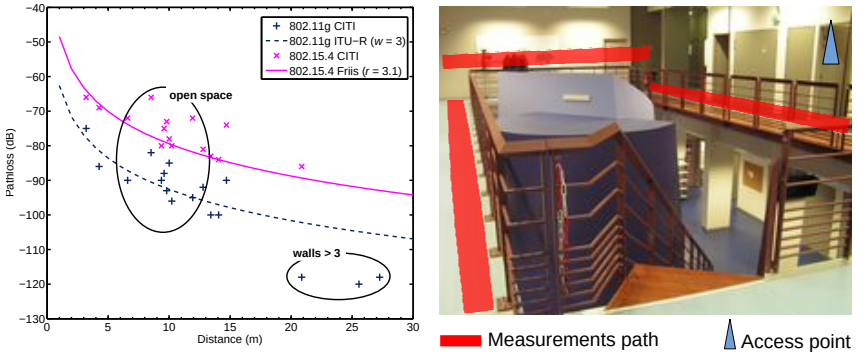

(a) Models vs Measurements (b) Measurements environment (CITI laboratory)

Figure 1: Pathloss channels models for 802.11g and 802.15.4: fit between the model used and the measurements (a) and (b) snapshot of the measurement environment

scattering, reflections... In multi-mode, channel conditions are different for each communication protocol. Hence, a signal transmitted in a mode m_j suffers a pathloss L_j.

In this work, we only consider the channel pathloss, as it represents the main component of channel conditions. We select different channel conditions for every mode, based on realistic and deterministic channel models. Pathloss follows dedicated propagation models in UMTS, 802.11g and 802.15.4.

Since, P_{out} depends on the channel conditions, we model the 802.11g, UMTS and 802.15.4 channels independently. We use the COST-Hata channel model in UMTS [10]:

$$\begin{aligned} L_{\text{UMTS}} =& 33.9\log_{10}(f) + \left(44.9 - 6.55\log_{10}(h_{BS})\right)\log_{10}(d) \\ &+ 46.3 - 13.82\log_{10}(h_{BS}) - a(h_{mobile}) + L_{scat} \end{aligned} \tag{4}$$

with L_{UMTS} the pathloss in line of sight (in dB), f the carrier frequency (in MHz), d (in km) the distance between the source and the transmitter, h_{BS} (in m) the height of the UMTS base station, h_{mobile} (in m) the height of the mobile terminal, L_{scat} (in dB) defining the scattering environment and $a(h_{mobile})$ the height correction factor, as specified by the model:

$$\begin{aligned} a(h_{mobile}) =& 1.1\log_{10}(f - 0.7)\cdot h_{mobile} \\ &- (1.56\log_{10}(f) - 0.8) \end{aligned} \tag{5}$$

We use an ITU-R office indoor channel model for 802.11g propagation [19]:

$$L_{\text{ITU-R}} = 20\log_{10}(f) + 30\log_{10}(d) - 28 + L_{wall}(w) \tag{6}$$

with $L_{\text{ITU-R}}$ being the pathloss (in dB), f the carrier frequency (in MHz), d the distance between two terminals, -28 the freespace loss coefficient and $L_{wall}(w) = 15 + 4(w-1)$ the penetration loss factor with w the number of walls penetrated.

We rely on a classical Friis model for 802.15.4 indoor propagation [21]:

$$L_{\text{Friis}} = r\left[10\log_{10}(f) + 10\log_{10}(d) + 10\log_{10}(\frac{4\pi}{C})\right] \tag{7}$$

Table 3: Parameters to consider in multi-mode energy evaluation

	802.11g		**UMTS**	**802.15.4**
Data bitrate – R	6 Mbps	54 Mbps	384 kbps	20 kbps
Processor energy consumption – E_{cpu} (nJ)	0.14	Identical for all modes, derived from [4] and (2)		
Radio front-end consumption – P_{frontend} (mW)				
Transmission	338 [6]		338 [6]	1 [30] +
Reception	198.8 [6]		198.8 [6]	1 [30] +
Transmission power output – P_{out} (dBm)				
Minimum	-20	-	-	-20
Maximum	10	-	-	0
Receiver sensitivity – $RXSens$ (dBm)	-87	-71	-106	-92
Pathloss model – L_j	ITU-R, $w = 3$ (6)		COST-Hata (4)	Friis, $r = 3.1$ (7)

+ [30] proposes an integrated 802.15.4 transceiver consuming 3.28mW in transmission and 3.29mW in reception. As we separate the numerical and radio consumptions, we reduce our front-end consumption to 1mW.

with L_{Friis} the indoor attenuation (in dB), f the carrier frequency (in Hz), d the distance between the two terminals (in m), C the speed of light, and r the pathloss exponent.

Fig. 1 presents the indoor measurements obtained at the CITI laboratory in 802.11g and 802.15.4 bands. These measurements permit the parametrization of the channel models with realistic conditions. As we can see on Fig. 1(a), we choose $w = 3$ for $L_{\text{ITU-R}}$ and $r = 3.1$ for L_{Friis}, respectively following (6) and (7). The low variations of measured attenuation, between 10 to 15 meters, is due to the inside architecture of our laboratory: a large open space surrounded by catwalks, as depicted on Fig. 1(b). We evaluate L_{UMTS} with (4) by setting $h_{BS} = 20$m, $h_{mobile} = 1.5$m, and $L_{scat} = 3$dB to represent a metropolitan environment. Since the mathematical models follows measurements, the pathloss values depend on the stated parameters throughout the rest of the paper.

4.4 Transmission power output evaluation

Terminals reduce their energy consumption by controlling their transmission power output, P_{out}. This technique, depending on the receiver sensitivity threshold ($RXSens$), will adapt P_{out} so that proper data decoding is possible at the receiver. Several existing methods allow the estimation of the channel conditions to reduce P_{out}, but this is not the scope of this paper. Here, we determine the transmission power, P_{out}, for a mode (m_j), as follows:

$$P_{\text{out}\,(dB)} = RXSens_j - L_j \quad (L_{j(dB)} < 0) \tag{8}$$

with L_j the pathloss (in dB) for mode m_j, referring to (4), (6) or (7), and $RXSens_j$ the receiver sensitivity (in dB) for mode m_j. $RXSens$ values depend on P_{frontend} specifications and are unique for each mode. The transmission power, P_{out}, is computed between two terminals after pathloss evaluation. P_{out} is then integrated into (3), in order to evaluate the radio energy consumption, E_{rf}. This process repeats for each selected communication mode.

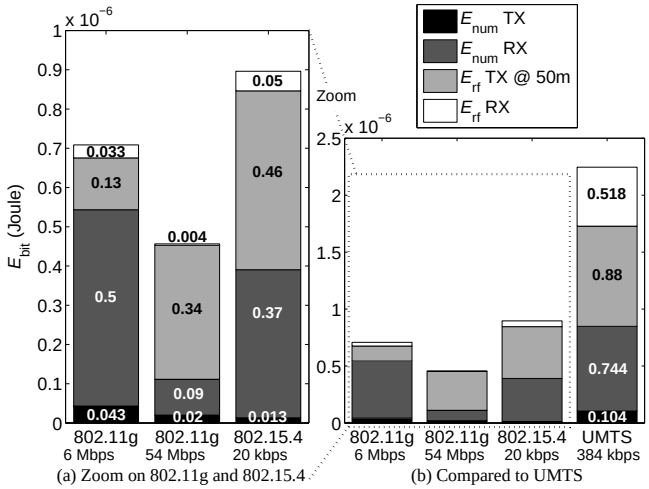

Figure 2: Detailed evaluation of E_{bit} (in Joule)

4.5 Parameters needed in multi-mode energy evaluation

In this section, we summarize the different parameters required to evaluate the energy consumption for a multi-mode terminal. Table 3 sums up these parameters and their values.

The processor energy consumption, E_{cpu} (in Joule), is the energy consumed by the processor to realize one operation. In this work, we consider an ARM 968E-S processor [4] running at one operation per cycle. From the specifications, we set the input voltage to $V_{dd} = 1.2$V, and assume $A_C = 97.3$pF (derived from the processor consumption reduced to one cycle). Thus, by setting K to the bitop value, we get E_{num} in Joule per bit for each mode following equation (2) and Table 2.

The radio front-end power, P_{frontend} (in Watt) denotes the power of the front-end during transmission or reception of an analog signal. In this work, we consider a multi-mode radio-frequency front-end, capable of receiving simultaneously signals in 802.11g, UMTS and 802.15.4. The front-end power for 802.11g and UMTS is the power of its low-level components, as evaluated in [6]. For 802.15.4, which requires a simpler circuitry, we derive values from [30]. Then, we integrate these values into equation (3), and recover the radio energy consumption E_{rf} (in Joule), for each mode with a bitrate R, as found in Table 1.

The receiver sensitivity, *RXSens* represents the minimum strength for a receiver to decode the signal accurately. The values presented here are based on typical values found in literature. Pathloss models, as introduced above, provide the channel conditions to adapt the transmission power, P_{out}, over a specified range.

4.6 Numerical evaluation of terminal energy consumption

In this section, we evaluate the required energy for a terminal to send and receive one single bit, E_{bit}, based on the previous sections.

Let us remember that the numerical energy consumption, E_{num}, remains constant at any distance, for a given protocol, at a given rate. The same pattern occurs for the radio energy consumption, E_{rf}, when ignoring the radio transmission power, P_{out}.

Indeed, P_{out} appears in transmission only, and remains the sole varying parameter when evaluating the radio energy consumption. As the distance increases, P_{out} is adjusted according to the receiver's channel conditions and distance, following equation (8). To obtain an estimation of E_{bit}, we evaluate P_{out} considering two users separated by a distance of 50 meters, for 802.11g, 802.15.4, and UMTS. We compute E_{num} from equation (2), using the numerical values presented on Table 2. We get E_{rf} values using equation (3), with the front-end consumptions values, P_{frontend}, taken from Table 3. The resulting values are represented on Fig. 2 for a communication between two terminals. The transmission power output, P_{out}, is set to its maximum value.

As expected from Table 2, Fig. 2(b) shows that UMTS at 384 kbps is the most consuming mode, far beyond other modes. In Fig 2(a), 802.11g at 6 Mbps has a higher energy efficiency than 802.11g at 54 Mbps. The "slow" 802.15.4 at 20 kbps has the second highest energy consumption. These considerations are relative to the chosen distance.

In all modes except 802.11g at 6 Mbps, we identify a higher E_{rf} than E_{num}. In UMTS, E_{rf} is almost twice E_{num}. This behaviour comes from the combination of a high P_{out} and a longer front-end activity needed to send or receive one bit. In 802.11g at 54 Mbps, the radio energy consumption is mainly determined by P_{out} because of the small receiver sensitivity (-71 dBm) combined with a strong attenuation for long distance (-113.6 dB). On the contrary, in 802.11g at 6 Mbps, E_{rf} is smaller than E_{num}, due respectively to the higher receiver sensitivity (P_{out} is smaller for this mode), and the more important bitop. In 802.15.4 at 20 kbps, the numerical and radio energy consumptions are almost identical when transmitting and receiving one data bit.

Let's now compare transmission and reception for each mode. At long distance, transmitting a bit is more expensive than its reception (for E_{rf}), due to P_{out}. However, we draw a different conclusion by considering E_{num} along E_{rf}: for 802.11g at 6 Mbps and UMTS at 384 kbps, their reception becomes predominant because of the numerical operations. Indeed, by looking at the different modes on their numerical part, we observe the predominance of the reception. This is true for all modes: the numerical reception used a lot of energy to process complex decoding and filtering operations, required to attain such rates. Hence, the energy consumed by the reception is only determined by the data bit rate, whereas the transmission behaviour mainly depends on P_{out} (at the considered distance). As the distance increases, P_{out} may rise very high. When the distance decreases, the radio transmission and reception become equivalent.

The consideration of both the numerical and radio part is clearly important in energy evaluation. Assuming the transmitter can vary its P_{out}, as the distance shortens, the transmission power output loses predominance. Ignoring E_{num} may give a wrong estimation. Moreover, these results also justify a per-bit approach for multi-mode energy evaluation. Indeed, the energy consumption of slow modes is higher than fast modes, for the same amount of data. Thus, the fact that slow equals "low-consumption" is generally wrong. On the contrary, we have shown that faster modes are likely to consume less energy due to their radio activity being the shortest.

5 Multi-mode relay to achieve energy reduction

5.1 Scenario presentation

In this section, we present the different scenarios used for energy evaluation. As mentioned before, three types of terminals are considered:

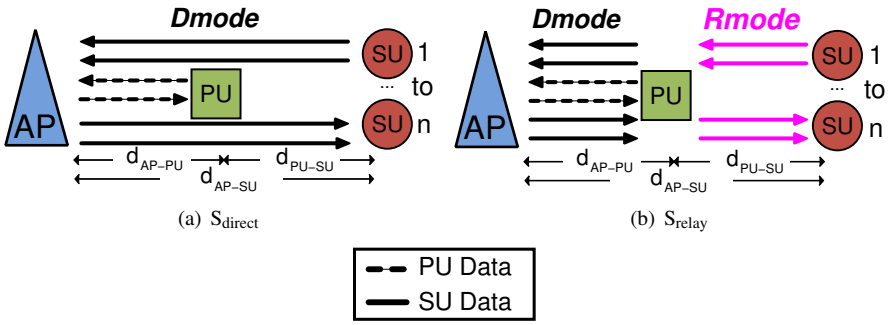

(a) S_{direct} (b) S_{relay}

Figure 3: Schematic representation of the scenarios studied

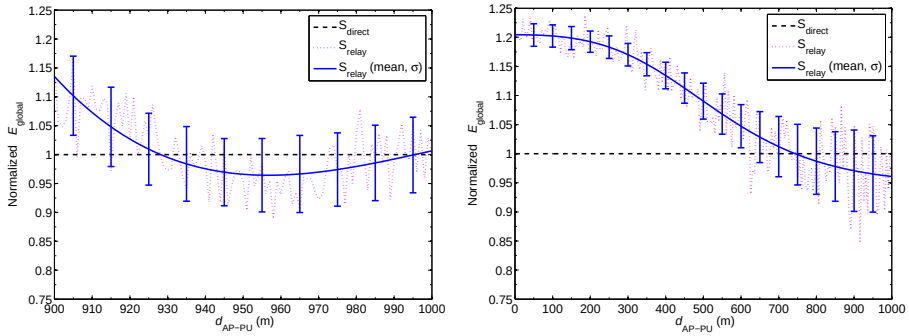

(a) PU mobile, SU fixed at $d_{AP-SU} = 1,000$m (b) PU and SU mobile, with fixed $d_{PU-SU} = 50$m

Figure 4: Comparison of energy per bit in various scenarios, normalized to scenario S_{direct}, in 802.11g-to-UMTS (one PU and one SU)

- A single Access Point (AP): a gateway with no energy constraints.
- A single Primary User (PU): a terminal directly connected to the access point and able to relay communications.
- *n* Secondary Users (SU): terminals relayed by the primary user *or* directly connected to the access point.

In these scenarios, illustrated in Fig. 3, AP communicates with PU or SU on a mode called the “Direct connection" mode (referred to as *Dmode*). The SU and the PU communicate with each other through a “Relayed connection" mode (referred to as *Rmode*).

In order to evaluate the gains of multi-mode relays, we compare the global energy consumption (*cf.* section 5.2) of the scenarios S_{direct} and S_{relay} denoted as:

- S_{direct}: PU and SU communicate directly in *Dmode*, as shown on Fig. 3(a).
- S_{relay}: PU acts as a relay and communicates with AP on *Dmode*. SU sends data to AP via PU on *Rmode*. PU establishes a new dedicated *Dmode* connection to AP, and relays SU’s data, as shown on Fig. 3(b).

5.2 Global energy consumption

We define the *global energy consumption*, E_{global} (in Joule), as the sum of all terminals' (except AP's) energy per bit.

$$E_{\text{global}} = \sum_{i=0}^{n} E_{\text{bit}}(i) \tag{9}$$

with $E_{\text{bit}}(i)$ the energy consumption of terminal i, and n the number of energy constrained terminals (PU or SUs). We decide to represent PU by $i = 0$, and SU_i, the different secondary users, by $i > 0$.

E_{bit} represents the consumption for one data bit, and it depends on the frame size and the number of hops. Hence, the number of bits sent for each useful data bit, denoted $\bar{b}$, is:

$$\bar{b} = \frac{S(f_j) + S(\text{MAC}_j)}{b_0} \tag{10}$$

with $S(\text{MAC}_j)$ the size of MAC layer control packets on mode j, $S(f_j) = b_j$ be the size of frame f on mode j, containing b_j bits, and b_0 be the initial data size.

Consequently, we express $\bar{b}$ for relayed packets as the sum of $\bar{b}$ for each link. For S_{relay}, we have:

$$\begin{aligned}\bar{b}(\text{S}_{\text{relay}}) = \frac{1}{b_0} \cdot \Big[& \alpha_{D\text{mode}} \big(S(f_{D\text{mode}}) + S(\text{MAC}_{D\text{mode}}) \big) \\ & + \alpha_{R\text{mode}} \big(S(f_{R\text{mode}}) + S(\text{MAC}_{R\text{mode}}) \big) \Big]\end{aligned} \tag{11}$$

with α_j, the number of fragmented packets in mode j to transmit b bits.

In the following sections, we evaluate E_{global} for the scenarios presented in section 5. If we denote $E_{\text{bit}}^{mode}(X,Y)$ the energy per bit spent by terminal X during his communication with Y on mode *mode*, we have the following formulae:

$$E_{\text{global}}(\text{S}_{\text{direct}}) = \sum_{i=1}^{n} E_{\text{bit}}^{Dmode}(\text{SU}_i, \text{AP}) + E_{\text{bit}}^{Dmode}(\text{PU}, \text{AP}) \tag{12}$$

$$\begin{aligned}E_{\text{global}}(\text{S}_{\text{relay}}) = & \sum_{i=1}^{n} E_{\text{bit}}^{Rmode}(\text{SU}_i, \text{PU}) + \sum_{i=1}^{n} E_{\text{bit}}^{Rmode}(\text{PU}, \text{SU}_i) \\ & + (n+1)\, E_{\text{bit}}^{Dmode}(\text{PU}, \text{AP})\end{aligned} \tag{13}$$

with $E_{\text{global}}(\text{S})$ the global energy consumption of scenario S in Joule, and $E_{\text{bit}}^{j}(i,\tau)$, the energy consumption per bit of terminal i on the selected mode j for a communication with terminal τ.

6 802.11g-to-UMTS simulations

In this section, we evaluate the energy consumption of an 802.11g-to-UMTS relay, with no interference, no control packets and no passive overhearing using Matlab simulations. The direct connection mode, *Dmode*, is UMTS at 384 kbps, and the relayed connection mode, *Rmode*, is 802.11g at 54 Mbps. We have implemented S_{direct} and

S_{relay} scenarios on Matlab, and compare their global energy consumption as presented on section 5.2.

Here, AP represents a UMTS base station, emitting to all its users. PU and SU are SDR terminals, with their energy consumption characterized by Table 2, Table 3 and Fig. 2 (as presented in section 4.6). For simplicity, AP, PU and SU are aligned and move along this alignment.

In UMTS, a signaling process is continuously emitted by AP and received by all terminals for power control. In order to simulate these signals fluctuations, we apply an independent fading to all communications. Since the terminals are all in line of sight, all signals suffer independent Rician fading, with standard deviation $\sigma = 0.5$, and $v = 1$. Moreover, we resorted to an uncapped P_{out}, so that long range line of sight 802.11g communications can occur.

6.1 Matlab simulations

The evaluation of $E_{bit}(SU_i, PU)$ depends on the distance between SU_i and PU, as presented on (12) and (13). In Matlab simulations, we consider all SUs approximately at the same distance from PU. Hence, these equations simplify as follows:

$$E_{global}(S_{direct}) \approx n\, E_{bit}^{Dmode}(SU_i) + E_{bit}^{Dmode}(PU) \tag{14}$$

$$E_{global}(S_{relay}) \approx n\, E_{bit}^{Rmode}(SU_i) + n\, E_{bit}^{Rmode}(PU) + (n+1)\, E_{bit}^{Dmode}(PU) \tag{15}$$

We evaluate the gains of relaying in the following topologies:

- PU moves from AP toward a single fixed SU.
- PU and a single SU are separated by a fixed distance, d_{PU-SU}, and move together from AP toward the cell border.
- PU moves from AP toward several fixed SUs, numbered from 1 to n.

Fig. 4 presents the global energy consumption, E_{bit}, normalized by $E_{global}(S_{direct})$, for one PU and one SU. It also shows the average values taken by S_{relay}, by representing its mean value and associated standard deviation, σ.

When the PU moves toward the SU, the distance between the AP and the SU is fixed at $d_{AP-SU} = 1,000$m. The distance between the PU and the SU, d_{PU-SU}, varies accordingly. Fig. 4(a) presents E_{global} for this topology, at a realistic communication range between PU and SU ($d_{PU-SU} \leq 100$m). The results show that S_{relay} brings less than 5% energy gains compared to S_{direct}, when PU is close to SU ($d_{PU-SU} \leq 70$m). At further distances, PU is too far from SU to consider relaying as a reliable solution: the transmission on *Rmode* is too expensive. Hence, direct connections should be prioratized, as the gains are null (or negative). Similarly, when PU is really close to SU ($d_{PU-SU} \leq 10$m), the mean E_{global} for S_{relay} is worse than S_{direct} because of the relay link. This behaviour reflects the equivalent energy consumption of UMTS connections.

In the case of fixed distance between PU and SU, we set $d_{PU-SU} = 50$m since this distance provides observable relaying gains. In this topology, PU and SU together move away from AP to reach the cell border. Fig. 4(b) shows that S_{relay} is meaningful when PU and SU move farther from AP ($d_{AP-PU} \geq 750$m), with increasing gains (with around 7% achievable near cell borders). However, the further both stations are from the AP, the higher the signal variations become.

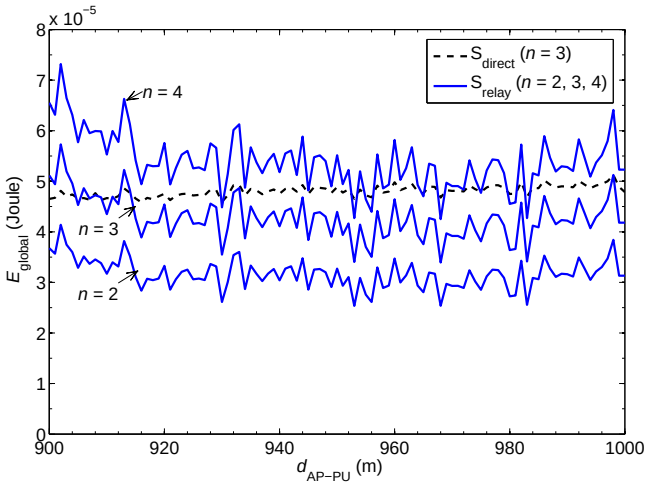

Figure 5: Normalized E_{global} in 802.11g-to-UMTS (one PU and n SUs)

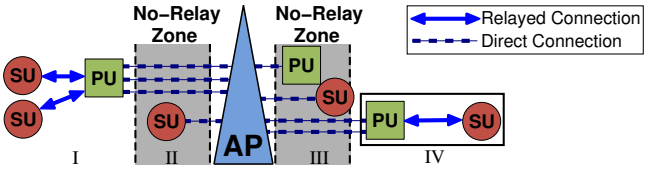

Figure 6: Relay rules for different terminals positions

For a moving PU relaying n fixed SUs, we considered all SUs near the cell borders. Fig. 5 shows the comparison of the global energy consumption of S_{direct} for $n = 3$ SUs, and S_{relay} for $n = 2,3,4$ SUs. According to the presented results (not normalized), E_{global} may have the same energy consumption for S_{relay} and S_{direct}, considering one more SU is relayed. This behaviour can happen when PU is near SU, when the channel conditions are favourable to the relay link.

6.2 Results summary

Based on the previous results, we define the "*No-Relay Zone*" as a zone where relaying brings no real gain compared to direct connections (we say less than 5%). When terminals are in the No-Relay Zone, they should prioratize direct connections. Outside the No-Relay Zone, terminals can decide to become a relay, or find a PU to be relayed.

Fig. 6 illustrates the following rules to minimize the global energy consumption, E_{global}. PU far from AP becomes a relay for the nearby SUs (Fig. 6 I), with gains of up to 7%. When PU and SU are close to each other, but near AP, they communicate directly with AP (Fig. 6 III). However, when they move together and reach the "No-Relay Zone", PU and SU can decide to keep relaying (Fig. 6 IV), with gains up to 7%. If the distance between PU and SU increases, they should contact AP directly. The same applies when PU and SU are in close proximity ($d_{\text{PU-SU}} < 10$m). Moreover, terminals close to AP should connect directly (Fig. 6 II).

By adding mobility, terminals acting as PU may relay one or several SUs for a certain period, before entering the “No-Relay Zone". At that moment, PU stops relaying and SU may choose another PU. SU can also become the PU for other terminals.

All other approaches which aim at energy reduction only consider the transmission power output and ignore the numerical energy consumption. We have shown how important this numerical energy consumption is in multi-mode, and we have explained how to minimize the global energy consumption using multi-mode relaying. In our work, any terminal following relay rules should limit its energy depletion in the long term. This way, by reducing a terminal energy consumption, we minimize the network global energy consumption.

7 802.15.4-to-802.11g simulations

In this section, we evaluate the energy consumption of an 802.15.4-to-802.11g relay. The direct connection mode, or *Dmode*, is 802.11g at 6 Mbps, and the relayed connection mode, or *Rmode*, is 802.15.4 at 20 kbps. For comparison purposes, we also evaluate a mono-mode relay, with *Rmode* set to 802.11g at 6 Mbps.

Here, AP represents an 802.11g access point at 6 Mbps, with no energy limit. As previously stated, PU and SU are SDR terminals, with their energy consumption characterized by Table 2, Table 3 and Fig. 2 (as presented in section 4.6). Their maximum transmission power, P_{out}, falls in the interval specified in Table 3.

We evaluate the global energy consumption of S_{direct} and S_{relay} in two different ways. First, we rely on Matlab simulations, using the same parameters as before (no control packet, no passive overhearing, no interference and no error). We show the limitations of Matlab simulations and introduce the need of a more realistic approach by using a network simulator. Then, we implement our scenarios in WSNet, a network simulator, considering control packets and passive overhearing, without interference or error. Recall that for a terminal in communication range, passive overhearing is the fact of receiving all incoming signals of a given mode, whether or not the terminal is the destination.

7.1 Matlab simulations

We first focus on Matlab simulations, with no control packet, or passive overhearing. The terminals are all aligned, and PU moves in straight line from AP to a fixed SU, located at $d_{\text{AP}-\text{SU}} = 30\text{m}$. We evaluate E_{global} following equation (14) and (15), for S_{relay} in multi-mode and S_{relay} in mono-mode with S_{direct} (for $n = 1, 3$). Fig. 7 presents the simulation results.

The gain of S_{relay} is null compared to S_{direct} for any *Rmode*: both relays almost double the global energy consumption of direct connections. By comparing multi-mode relay with mono-mode relay, S_{relay} with *Rmode* 802.15.4 at 20 kbps is only improved by 5% to 10%. Moreover, mono-mode relay with *Dmode* 802.11g at 6 Mbps connections gives no advantage over direct connections. For a single moving PU, we conclude that a relay brings no gain on the global energy consumption using these assumptions.

In case of multi-users relayed by a mobile PU, the establishment of a dedicated connections presents critical losses, as shown on Fig. 7. Relay gains are deteriorating as n increases: direct connections for $n = 3$ is almost as energy efficient as relaying one single SU. These energy consumptions come from the highest cost of concurrent

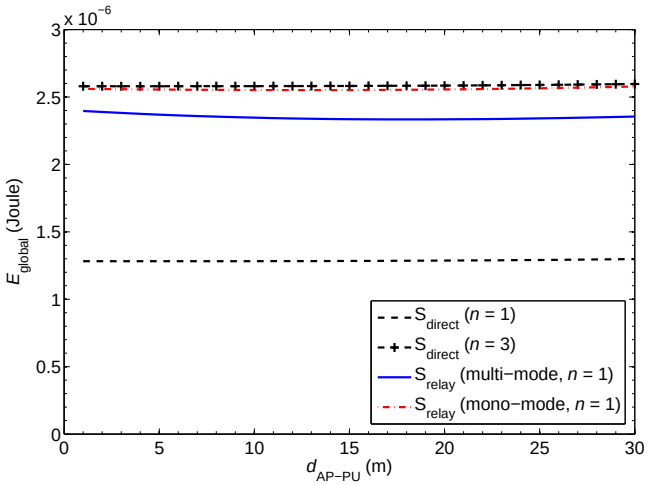

Figure 7: Comparison of the energy per bit of direct and relayed communication for a 802.15.4 to 802.11.g relay, using Matlab simulations

802.11g connections, and the greater radio consumption of multiple 802.15.4 links at middle and long range.

7.2 Network simulations for a better precision

Since Matlab simulations only present an analytical point of view, we rely on network simulations to study a more realistic behaviour. We choose WSNet, a realistic sensor network simulator developed at the CITI laboratory, with cross-layer capabilities [9].

WSNet can simulate several Medium Access Control layers (MAC) protocol, in particular, the protocols 802.11g and 802.15.4 that we have simulated in Matlab. Although a MAC layer defines rules for fair medium sharing between all users, this process remains local between a source (sending data), and a destination (receiving these data).

Both 802.11g and 802.15.4 implement Carrier Sense Multi-user Access (CSMA), with Collision Avoidance (CSMA/CA) in 802.11g. In CSMA, a particular source first listens to the medium before sending data. If the channel is free, the source sends its data. Otherwise, the source starts a random back-off timer: a waiting time before listening again. The process repeats until all data is sent or discarded. After correct reception, the destination replies with an Acknowledgement packet (ACK) to the source.

The peculiarity of the CSMA/CA protocol comes from control packets. When the medium is free, the source sends a Request To Send packet (RTS) at full transmission power, asking the destination if data reception is possible. If the destination is neither in transmission, nor receiving data from other users, a Clear To Send packet (CTS) is replied and normal communication can take place.

In this section, the energy consumption is evaluated using equation (12) and (13).

7.3 WSNet simulations

In this section we focus on the uplink of every scenario (PU and SU send data to AP). The transmission power of control packets is not limited, and AP always transmits at

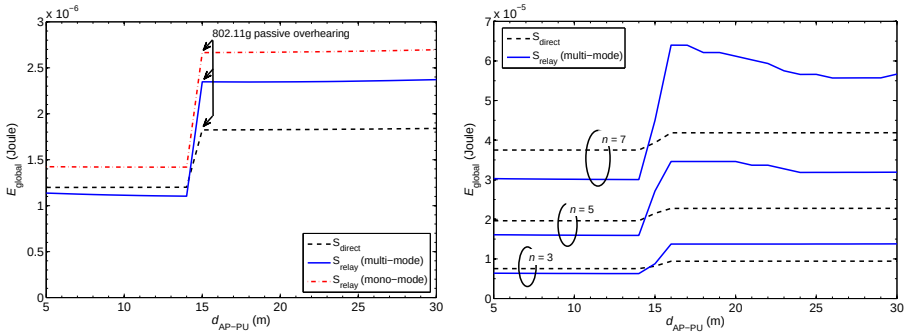

(a) $n = 1$ (b) $n = 3, 5, 7$

Figure 8: Comparison of energy per bit for direct or 802.15.2-to-802.11g relayed communication for n SUs, in uplink using WSNet simulations.

Table 4: WSNet simulation settings

	802.11g	**802.15.4**
Parameters controllable in WSNet		
Data bitrate – R	6 Mbps	20 kbps
MAC layer	CSMA/CA	CSMA
Frame size (bytes) – $S(f_j)$	500	500
Parameters independent from WSNet		
Control packets size (bytes)	RTS: 36, CTS: 28, ACK: 26	-
Cumulative headers size (bytes) – $S(MAC_j)$	84	40

the maximum allowed power. By default, passive overhearing is active on all modes (terminals receive data from other users in range). We evaluate the global energy consumption, E_{global}, for S_{direct} and S_{relay}.

We simulate the same scenario: a moving PU and fixed SUs. The distance between SUs and AP remains the same. Thus, n SUs are placed 2.5m apart from each other, on a circle centered on AP (radius $d_{\text{AP-SU}} = 30$m). PU moves from $d_{\text{AP-PU}} = 5$m (approximately the maximum transmission distance of 802.15.4 in the selected conditions) toward these n SUs. Table 4 presents the implemented parameters in WSNet simulations. $S(f_j)$ is the frame size for mode m_j. $S(MAC)$ represents the cumulative size of all headers, from the application to MAC layer included. All data frames have the same original size, $b_0 = 500$bytes, and control packets are only used in 802.11g. Terminals parameters come from Table 3, as previously.

Fig. 8 presents the evaluation of E_{global} after WSNet simulations, focusing on the uplink. We notice a “jump" happening exactly when PU is halfway between AP and SUs ($d_{\text{AP-PU}} = 15$m). Indeed, when PU moves closer to SU(s) than AP, the increasing transmission power leads all SUs to receive the 802.11g signal.

For comparison purposes, Fig. 8(a) also presents the results of S_{relay} in mono-mode (802.11g-to-802.11g relay), for one relayed SU. In Fig. 8(a) we see that that E_{global} is almost equivalent for both relays and direct connections.

When PU is near AP, a multi-mode relay consumes only 5 to 7% less energy than S_{direct}. After the jump, the consumption of multi-mode relay deteriorates by 28% com-

pared to direct connections. In case of mono-mode relay, E_{global} deteriorates by 18% and 45% compared to S_{direct}, before and after the jump respectively. When there is only one SU, relaying is useless.

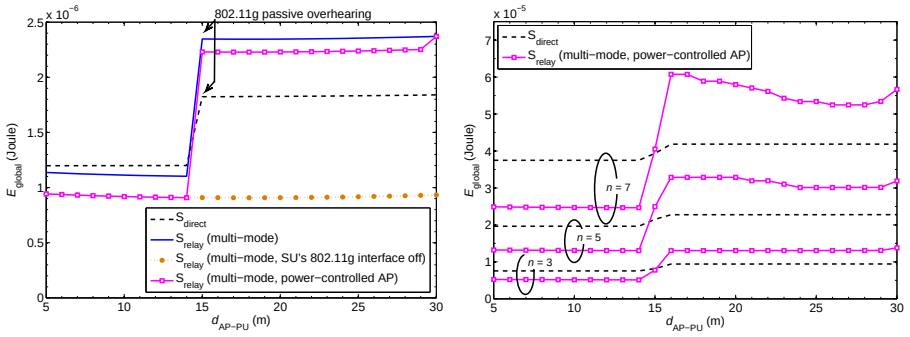

(a) $n = 1$ (b) $n = 3,5,7$

Figure 9: Comparison of energy per bit for direct or 802.15.2-to-802.11g relayed communication for n SUs, in uplink using WSNet simulations, including 802.11g deactivation and power-controlled transmission

Fig. 8(b) presents E_{global} for $n = 3,5$ and 7 SUs. In this case, passive overhearing appears in both modes of S_{relay}: in 802.15.4 at all times, and in 802.11g after the jump (when PU comes near SUs). Moreover, all terminals suffer from passive overhearing from their neighbours in S_{direct} (*e.g.* PU receives signals from all SUs). Note that AP always transmits at full power, thus all SUs receive control packets emitted by AP. As explained before, when PU is close to AP, the 802.11g signal in S_{relay} does not reach SU. Hence, the consumption of S_{relay} becomes more interesting with n before the jump: 15% better for $n = 3$, 20% better for $n = 7$ SUs. However, after the jump, PU rises its P_{out} so that its signal can reach AP. Consequently, all SUs receive the data transmitted by PU, and S_{relay} consumption keeps increasing with n. For $n = 7$ SUs, S_{relay} consumes around 35% more energy than direct connections. The decreasing part after the "jump" is due to the topology in circle.

The results presented on Fig. 8(b) show a marginal interest of multi-mode relay compared to direct connections. Although these results were expected from Matlab simulation, they are confirmed with a more realistic simulation. After implementing the same scenarios with more refined parameters on WSNet, S_{relay} energy consumption still remains close to the energy consumption of direct connections.

Even though E_{rf} is higher in 802.15.4, it cannot explain by itself the high different in E_{global} with multiple long range 802.11g connections. This leads us to consider different parameters influencing the energy consumption: control packets and passive overhearing.

In the next section, we quantify the gains of these two different approaches on relaying for the same scenarios.

7.4 Network simulations with 802.11g-deactivation and power-controlled transmission

As presented previously in section 7.2, WSNet simulations permits one to observe the influence of passive overhearing (terminals receive data emitted by their neighbours)

and control packets (linked to the MAC layer) on the network global energy consumption, E_{global}. In this section, we show how these two factors influence the global energy consumption. We evaluate two solutions to reduce E_{global} in a multi-mode S_{relay}. A first approach is to limit the transmission power of AP regarding PU's position. This limitation applies to all signals transmitted by AP. The second solution is to disable SU's 802.11g interface to ignore passive overhearing on the inactive interface. In this case, denoted hereafter "S_{relay} with inactive 802.11g interface", all costs linked to the 802.11g interface are removed, and 802.15.4 overhearing occurs for SUs. In both cases, PU transmits control packets at full power, to prevent hidden terminals effect.

Fig. 9 presents an evaluation of E_{global} in uplink, for S_{direct} and multi-mode S_{relay}. Fig.9(a) shows the impact of control packets. When AP's control packets are limited to PU, the energy gains are 17% better than S_{relay} (only before the jump). After the jump, this solution remains 5% better than S_{relay}. However, direct connections are still preferable after the jump, mostly due to passive overhearing on the inactive interface.

Fig.9(a) also shows that deactivating SU's 802.11g interface drastically reduces the global energy consumption after PU reaches the midway point (S_{relay} energy consumption is around 50% better than S_{direct}). Before the jump, the energy consumption remains at the same level of a power-controlled AP, due to the high 802.15.4 P_{out}.

For n SUs, we choose to represent S_{direct} and S_{relay} with a power-controlled AP on Fig. 9(b). Indeed, the energy consumption of S_{relay} with SU's 802.11g interface deactivated has small variations: its values follow the behaviour of S_{relay} with a power-controlled AP before the jump. We show that when PU is close to AP, energy reduction increase with n for S_{relay} (around 30% gains for $n = 3$, up to 35% for $n = 7$). Still, when PU reaches midpoint, the cost of 802.11g passive overhearing makes S_{relay} global energy consumption larger than S_{direct} (around 40% for $n \geq 3$). However, the decreasing curve for $n = 7$ comes from the positioning of the SUs, which limit their P_{out} to communicate with PU (SUs too far away do not receive the signal).

The two solutions presented here allow the reduction of the global energy consumption to a certain extent. When deactivating the passive interface for relayed users, a multi-mode terminal works as a mono-mode one. The energy consumption is greatly reduced when PU comes too close to the SU, since passive overhearing is ignored. However, this solution might introduce problems: terminals lose their multi-mode properties. As a solution, the 802.15.4 can be used as a wake-up radio (when a certain signal is received, the terminal activates its inactive interface). Or the terminal can rely on random or scheduled sensing, to determine whether keeping this scheme, becoming a PU, or use a direct connection with AP.

Power-constrained transmission allows reduction of the global energy consumption, while not suffering from the disadvantages of 802.11g-deactivation at the SUs'. Compared to direct connections, this relay provides a lower cost and good coverage for all users but only when PU is near AP and for a high number of relayed users ($n \geq 5$). However, the problem of the hidden terminal remains. Hence, a new terminal must send a request to be detected, while PU should respond at full power during a very limited time. The new terminal might also be reported to AP by PU, if its maximum power is not sufficient. Moreover, current SUs might check the quality of their connection with AP: terminals can rely on a negotiation protocol established through the relay link, and ask AP to transmit at full power.

8 Discussion and conclusions

As we have seen, the 802.11g-to-UMTS relay brings noticeable gains when PU is moving toward several SUs: between 10% and 15% on average. However, this scheme is subject to a "No-Relay Zone" where minimal gains occur. In 802.15.4-to-802.11g relay, the deactivation of SU's 802.11g interface provide up to 50% in energy reduction by removing passive overhearing. Yet, several problems may arise with the deactivation of multi-mode (*i.e.* when new terminals arrive in the network). The energy consumption of multi-mode mobile relays depends on the different parameters detailed through realistic simulations. Each of these parameters must be carefully examined before taking any decision. Their impact on relaying is important, and some intuitive solutions do not provide a positive result and therefore shall not be implemented, as explained as follows:

- Control packets: when using a realistic MAC layer, control packets specify when to access the medium. They also acknowledge good data reception. These packets must be taken into account when evaluating the energy requirements of a mode. We have shown their importance by comparing Matlab and WSNet simulations. Moreover, their passive overhearing by secondary users leads to a higher global energy consumption than direct connections.

- Access Point transmission power: the limitation of the transmission power to only reach PU might lead to energy savings. However, when limited, a hidden terminal problem might occur. When a SU wants to communicate on *Dmode*, it will not receive any control packets. This leads to probable collisions. We could prevent this by using a power controlled AP coupled with on-demand access by SU.

- Multi-mode overhearing: disabling the *Dmode* interface at the relayed users' side should lead to better efficiency. Nevertheless, the multi-mode capacity is lost, and mono-mode overhearing still occurs with the same protocol. Such measures require periodic listening on the *Dmode* interface, to verify if the relay still provides more energy gains than direct connections. Another measure might be to send a wake-up signal on the active interface. This solution is preferred for relaying multiple users with a very low energy consumption.

- Number of users: the more secondary users are relayed, the higher the cost of passive overhearing becomes. This passive overhearing happens on *Dmode* and on *Rmode*. While considering *Dmode* overhearing, disabling this interface at the SUs might be a solution. However, such a technique is not always possible when dealing with multi-mode. A better solution requires an adapted MAC layer. A slotted MAC layer (such as TDMA) could answer these critics, though it introduces an increasing delay related to the number of SUs. Evaluation of the optimal number of relayed users per PU is the solution, but this is not the scope of this paper.

In this paper, we have presented a model to evaluate the energy consumption of multi-mode terminals. This model considers not only the radio energy and the transmission power output, but also includes the numerical energy consumption. We have carried out realistic network simulations of simple scenarios, and have evaluated the global energy consumption of multi-mode relays. Contrary to common belief, relays deployment may not always lead to a drastic reduction in energy consumption. Our

conclusions highly depend on the chosen parameters: numerical architecture, algorithm implementation, radio front-end, channel conditions and scenarios.

Since every one of these parameters is important when relaying, we have developed the necessary tools to evaluate the energy consumption of all these components (from the terminal to the network). It is certain that some terminals may benefit from relay, but the global energy consumption highly depends on the aforementioned factors. Indeed, relaying can be an energy saver for the network, but only when some specific conditions are met. The energy consumption for other scenarios and under different channel conditions may present different results. Especially in multi-mode, where the modes chosen are influenced by these parameters, and passive overhearing on the inactive modes draws a large energy consumption.

We have shown that “low-power" modes are not that interesting when considering their energy per bit. Terminals using such modes should deal with an increased complexity: the computational costs of “low-power" modes (*i.e.* Zigbee) requires more energy than 54 Mbps in 802.11g.

In conclusion, energy reduction remains crucial in mobile networks. It may be reached by combining all the possible energy gains. For a terminal, new architectures are taking energy efficiency seriously (be they numerical or radio). In parallel, the development of more efficient algorithms will lead to additional energy gains. Our tools allow us to evaluate the impact of new solutions on the energy consumption, from the terminal to the network.

References

[1] 3rd Generation Partnership Project. UMTS Physical layer procedures (TDD) (Release 8). http://www.3gpp.org/ftp/Specs/html-info/25224.htm, March 2008.

[2] Federico Albiero, Frank H.P. Fitzek, and Marco Katz. Cooperative power saving strategies in wireless networks: an agent-based model. In *Wireless Communication Systems, 2007. ISWCS 2007. 4th International Symposium on*, pages 287–291, Oct. 2007.

[3] Federico Albiero, Marco Katz, and Frank H.P. Fitzek. Energy-efficient cooperative techniques for multimedia services over future wireless networks. In *Communications, 2008. ICC '08. IEEE International Conference on*, pages 2006–2011, May 2008.

[4] ARM Processor. ARM 968 E-S processor. http://www.arm.com/products/CPUs/ARM968E-S.html, consulted on July 2010.

[5] Lars Berlemann, Ralf Pabst, and Bernhard Walke. Multimode communication protocols enabling reconfigurable radios. *EURASIP J. Wirel. Commun. Netw.*, 2005(3):390–400, 2005.

[6] Ioan Burciu, Matthieu Gautier, Guillaume Villemaud, and Jacques Verdier. A 802.11g and UMTS Simultaneous Reception Front-End Architecture using a double IQ structure. In *Proceedings of the IEEE 69th Vehicular Technology Conference (VTC '09)*, Barcelona, Spain, April 2009.

[7] Dave Cavalcanti, Nagesh Nandiraju, Deepti Nandiraju, Dharma P. Agrawal, and Anup Kumar. Connectivity opportunity selection in heterogeneous wireless multi-hop networks. *Pervasive and Mobile Computing*, 4(3):390 – 420, June 2008.

[8] Damien Charlet, Valérie Issarny, and Rafik Chibout. Energy-efficient middleware-layer multi-radio networking: An assessment in the area of service discovery. *Comput. Netw.*, 52(1):4–24, 2008.

[9] Guillaume Chelius, Antoine Fraboulet, and Elyes Ben Hamida. WSNet – An event-driven simulator for large scale wireless sensor networks. http://wsnet.gforge.inria.fr/, 2008.

[10] Dieter J. Cichon and Thomas Kürner. Cost 231 Final Report – Chapter 4: Propagation Prediction Models. http://www.lx.it.pt/cost231/final_report.htm, 1998.

[11] Björn Debaillie, Bruno Bougard, Gregory Lenoir, Gerd Vandersteen, and Francky Catthoor. Energy-scalable ofdm transmitter design and control. In *Proceedings of the 43rd annual conference on Design automation (DAC '06)*, pages 536–541, San Francisco, CA, USA, July 2006.

[12] G. Ganesan and Y. Li. Cooperative Spectrum Sensing in Cognitive Radio, Part I: Two User Networks. *IEEE Transactions on Wireless Communications*, 6(6):2204–2213, June 2007.

[13] O. Holland, M. Muck, P. Martigne, D. Bourse, P. Cordier, S. Ben Jemaa, P. Houze, D. Grandblaise, C. Klock, T. Renk, et al. Development of a Radio Enabler for Reconfiguration Management within the IEEE P1900. 4 Working Group. In *Proceedings of the 2nd IEEE International Symposium on New Frontiers in Dynamic Spectrum Access Networks (DySPAN '07)*, pages 232–239, Dublin, Ireland, April 2007.

[14] Kyu-Sung Hwang and Young-Chai Ko. An efficient relay selection algorithm for cooperative networks. In *Vehicular Technology Conference, 2007. VTC-2007 Fall. 2007 IEEE 66th*, pages 81–85, 30 2007-Oct. 3 2007.

[15] IEEE Computer Society. 802.11g part 11: Wireless lan medium access control (mac) and physical layer (phy) specifications. http://standards.ieee.org/getieee802/download/802.11g-2003.pdf, June 2003.

[16] IEEE Computer Society. IEEE Std 802.15.4?-2006 Part 15.4: Wireless Medium Access Control (MAC) and Physical Layer (PHY) Specifications for Low-Rate Wireless Personal Area Networks (WPANs). http://standards.ieee.org/getieee802/download/802.15.4-2006.pdf, September 2006.

[17] IEEE Standards Coordinating Committee 41 (Dynamic Spectrum Access Networks). http://grouper.ieee.org/groups/scc41/, February 2009.

[18] Joe Inwhee, Kim Won-Tae, and Hong Seokjoon. A network selection algorithm considering power consumption in hybrid wireless networks. *IEICE Transactions*, 91-B(1):314–317, 2008.

[19] ITU Radiocommunication Assembly. Recommendation ITU-R P.1238-1 : Propagation data and prediction models for the planning of indoor radiocommunication systems and radio local area networks in the frequency range 900 MHz to 100 GHz, October 1999.

[20] Peng Jiang, John Bigham, and Jiayi Wu. Self-organizing relay stations in relay based cellular networks. *Computer Communications*, 31(13):2937 – 2945, August 2008.

[21] Kari Laasonen. Radio propagation modeling. Technical report, University of Helsinki, 2003.

[22] Han Yong Lee, Winston K.G. Seah, and Peng Sun. Energy implications of clustering in heterogeneous wireless sensor networks - an analytical view. In *Personal, Indoor and Mobile Radio Communications, 2006 IEEE 17th International Symposium on*, pages 1–5, Sept. 2006.

[23] R. Madan, N. Mehta, A. Molisch, and Jin Zhang. Energy-efficient cooperative relaying over fading channels with simple relay selection. *Wireless Communications, IEEE Transactions on*, 7(8):3013–3025, August 2008.

[24] Jody Neel, Jeff Reed, and Max Robert. A formal methodology for estimating the feasible processor solution space for a software radio. In *Proceedings of the Software Defined Radio Technical Conference and Product Exposition (SDRForum '05)*, Orange County, CA, USA, November 2005.

[25] H. Nourizadeh, S. Nourizadeh, and R. Tafazolli. Performance evaluation of cellular networks with mobile and fixed relay station. In *Proceedings of the 64th IEEE Vehicular Technology Conference (VTC '06)*, Montréal, Canada, September 2006.

[26] Gerard K. Rauwerda, Paul M. Heysters, and Gerard J. M. Smit. Mapping wireless communication algorithms onto a reconfigurable architecture. *J. Supercomput.*, 30(3):263–282, 2004.

[27] K. G. Seddik, A. K. Sadek, W. Su, and K. J. R. Liu. Outage Analysis and Optimal Power Allocation for Multinode Relay Networks. *IEEE Signal Processing Letters*, 14:377–380, June 2007.

[28] Eugene Shih, Seong-Hwan Cho, Nathan Ickes, Rex Min, Amit Sinha, Alice Wang, and Anantha Chandrakasan. Physical layer driven protocol and algorithm design for energy-efficient wireless sensor networks. In *Proceedings of the 7th annual international conference on Mobile computing and networking (MobiCom '01)*, pages 272–287, Rome, Italy, July 2001.

[29] A. Wang and A. Chandrakasan. Energy-efficient DSPs for wireless sensor networks. *Signal Processing Magazine, IEEE*, 19(4):68–78, July 2002.

[30] Chua-Chin Wang, Jian-Ming Huang, Chih-Yi Chang, Kuang-Ting Cheng, and Chih-Peng Li. A 6.57 mw zigbee transceiver for 868/915 mhz band. In *Circuits and Systems, 2006. ISCAS 2006. Proceedings. 2006 IEEE International Symposium on*, pages 4 pp.–5198, 0-0 2006.

[31] Wei Wang, Vikram Srinivasan, and Kee-Chaing Chua. Extending the lifetime of wireless sensor networks through mobile relays. *IEEE/ACM Transactions on Networking*, 16(5):1108–1120, October 2008.

Centre de recherche INRIA Grenoble – Rhône-Alpes
655, avenue de l'Europe - 38334 Montbonnot Saint-Ismier (France)

Centre de recherche INRIA Bordeaux – Sud Ouest : Domaine Universitaire - 351, cours de la Libération - 33405 Talence Cedex
Centre de recherche INRIA Lille – Nord Europe : Parc Scientifique de la Haute Borne - 40, avenue Halley - 59650 Villeneuve d'Ascq
Centre de recherche INRIA Nancy – Grand Est : LORIA, Technopôle de Nancy-Brabois - Campus scientifique
615, rue du Jardin Botanique - BP 101 - 54602 Villers-lès-Nancy Cedex
Centre de recherche INRIA Paris – Rocquencourt : Domaine de Voluceau - Rocquencourt - BP 105 - 78153 Le Chesnay Cedex
Centre de recherche INRIA Rennes – Bretagne Atlantique : IRISA, Campus universitaire de Beaulieu - 35042 Rennes Cedex
Centre de recherche INRIA Saclay – Île-de-France : Parc Orsay Université - ZAC des Vignes : 4, rue Jacques Monod - 91893 Orsay Cedex
Centre de recherche INRIA Sophia Antipolis – Méditerranée : 2004, route des Lucioles - BP 93 - 06902 Sophia Antipolis Cedex

Éditeur
INRIA - Domaine de Voluceau - Rocquencourt, BP 105 - 78153 Le Chesnay Cedex (France)
http://www.inria.fr
ISSN 0249-6399